Surface modification with the scanning tunneling microscope

by David W. Abraham H. Jonathon Mamin Eric Ganz John Clarke

We describe the design and operation of a scanning tunneling microscope (STM) intended for studying surfaces. We are able to prepare samples with ion bombardment and heating, and to characterize them with LEED and Auger analysis in situ before scanning with the STM. Data acquisition and analysis are computercontrolled, with a wide variety of options for presentation. In the near future, we will be able to load-lock samples without venting the UHV chamber. Our STM has very low thermal drift, typically of the order of 1 Å/min. In addition to topographical measurements of the surface, we have obtained spatially resolved maps related to the height of the tunnel barrier. We have investigated the effects of scratching the surface with the tip, and have also succeeded in depositing material from the tip onto the surface. Surface diffusion of material is found to play an important role in both of these processes.

[®]Copyright 1986 by International Business Machines Corporation. Copying in printed form for private use is permitted without payment of royalty provided that (1) each reproduction is done without alteration and (2) the *Journal* reference and IBM copyright notice are included on the first page. The title and abstract, but no other portions, of this paper may be copied or distributed royalty free without further permission by computer-based and other information-service systems. Permission to *republish* any other portion of this paper must be obtained from the Editor.

1. Introduction

Until the development of the scanning tunneling microscope (STM) in 1983 [1], microscopy at the atomic level was limited to electron-beam machines with poor resolution in the vertical dimension [2], and to the field-ion microscope, which is limited to a small set of materials under high electric fields [3]. With the advent of the STM, however, atomic-resolution microscopy on a large class of electrically conductive materials has become feasible in most laboratories.

We briefly describe our own version of the STM, which we have designed to minimize long-term drift and to enable us to move samples to other parts of the UHV chamber for surface treatment and characterization. A variety of different modes for displaying the data have been investigated. Our STM has been operated simultaneously in a "topographical mode" and a "barrier height mode." We also report preliminary experiments in which we modify the surface under study using the probe tip, and then use the same tip to monitor the changes induced. Indentations and hillocks have been created with sizes on a 100-Å scale, and we have observed surface diffusion as these features evolve toward stable configurations.

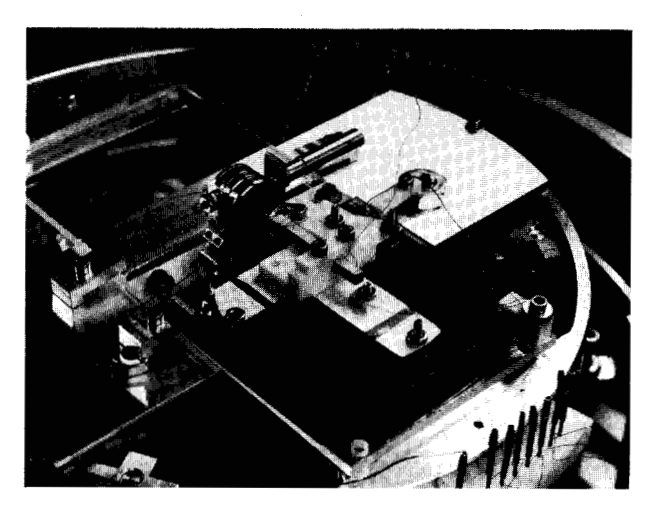
2. Description of the instrument

Our STM is shown in Figure 1. The sample is mounted on a cylindrical molybdenum stub. (In a later version, the sample

is held on the front surface of the stub by spring clips, thereby facilitating cleaning by ion bombardment.) In operation, the stub is placed in the U-shaped holder and is held in place with a spring-loaded bullet. The body of the microscope is made of quartz, which provides low thermal drift of the tip with respect to the sample. To form an image, we scan the sample in the x- and y-directions by means of orthogonal piezoelectric transducers extending down from the U-shaped holder. The probe tip, which consists of a mechanically ground 1-mm-diameter tungsten wire, is attached to the piezoelectric z-drive, and the assembly is mounted on our walker [4], which we use to bring the tip-tosample distance to within the dynamic range of the z-drive. Our walker is made from a single piece of piezoelectric material, and has three feet and two extension regions for motion in two directions. The feet of the walker are ground flat and coated with a Cr metallizing film followed by an insulating layer of SiO. The walker moves on an optically flat quartz plate that has been similarly coated.

This configuration offers a number of advantages. First, since there are no wires attached to the sample, it can readily be inserted into and removed from the microscope. Electrical contact is made when the sample is placed into the U-shaped holder which is mounted rigidly on the x- and y-drives. Second, the z-drive is mechanically separated from the x- and y-drives. Thus, the lowest-frequency mechanical resonance excited by the feedback system depends only on the z-drive, and is independent of the length of the x- and y-drives. By changing the length of the z-drive we can trade off response frequency against dynamic range. This allows the use of a short, fast z-drive as well as long, larger-range xand y-drives. The microscope is mounted at the top of a two-stage vibration isolation system suspended from springs and damped with samarium-cobalt magnets and copper blocks. To damp high-frequency vibration, we use viton O-rings to attach the springs to the system. The entire microscope is mounted in a Varian ion-pumped ultrahighvacuum system with a conventional surface-science bell jar. After bakeout, the system achieves pressures down to 1 × 10⁻¹⁰ torr. The residual gas can be analyzed with a highresolution mass spectrometer. The sample can be removed from the STM and transferred in UHV to a manipulator for preparation with electron-beam heating and ion-beam sputtering, and analysis with LEED and retarding-field Auger. We are currently incorporating a UHV load-lock system that will allow us to change samples without venting the UHV system.

The microscope is operated with a constant voltage bias between the tip and the sample. The current is monitored with a current-to-voltage converter followed by several stages of amplification, in general a logarithmic amplifier, a single-pole integrator, and an output stage that consists of a (slow) high-voltage amplifier driving one electrode of the z-drive and a (fast) ± 15 -V amplifier driving the other. We have successfully used both linear feedback circuits and ones



Photograph of experimental arrangement. Sample is mounted in the U-shaped holder in the center of the apparatus and can be removed for preparation and analysis elsewhere in the vacuum system. The T-shaped walker is used for coarse positioning of the tip with respect to the sample.

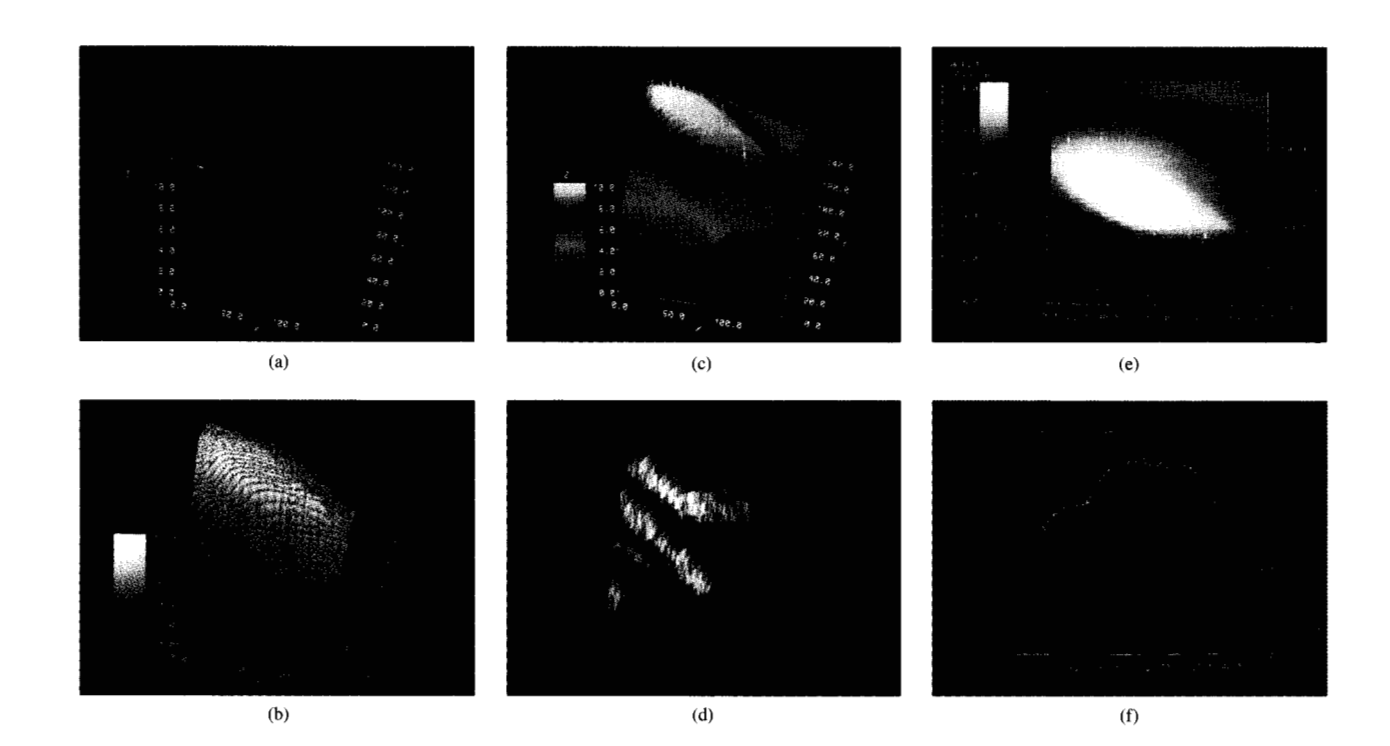
containing a logarithmic amplifier. The logarithmic amplifier linearizes the exponential response of the current to a change in tip-to-sample spacing. Of course, for a small error signal, the linear system is equivalent to the logarithmic system. But for fast scan rates on coarse surfaces where the error signal may be large, we prefer the logarithmic system, since the slew rate is nearly symmetric for extension or retraction of the tip. On the other hand, for work on smooth surfaces, the linear system avoids drifts inherent in logarithmic amplifiers, and simplifies the electronics at the expense of a slower response when the feedback extends the tip towards the surface.

Data are collected with a DEC LSI 11/23 computer which displays each row of data as it is taken. The sample is scanned using two analog ramp voltage generators, while the computer samples 60 to 120 rows of 256 points each. Typically, we run the x-ramp at a few seconds per row, while the y-ramp completes a scan in a few minutes. We can present the data in the form of rotated wire-frame plots within one minute of completing a series of scans. We have found it invaluable to be able to perform software manipulations of the data, such as rotations and scale changes, immediately after taking a picture to give us guidance for the next series of scans. The computer is also used to control the motion of the walker, monitor the status of the feedback loop, and trigger and reset the analog ramps.

3. Data display

For more sophisticated modes of display, we transfer the data to a Tektronix 4115B color graphics workstation. This





Examples of displays of data obtained from polished <210> surface of gold crystal: (a) projected line plot, (b) gray-scale fill plot, (c) color fill plot, (d) light-sourced image, (e) top view, and (f) single data scan indicated by arrow in (a). Scales are in Å.

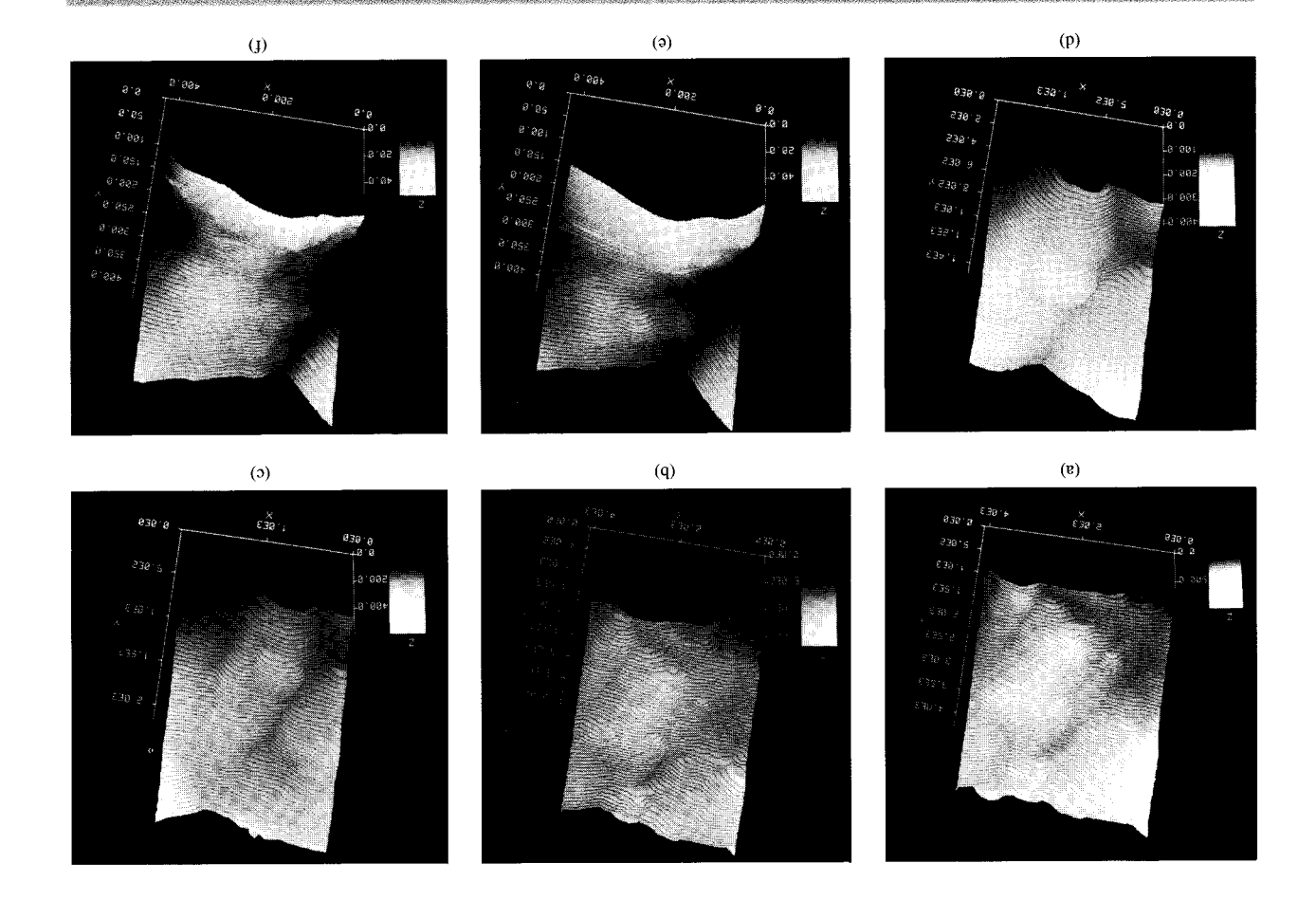
computer has a screen resolution of 1024×1280 pixels, with up to 256 colors. Examples of various output formats are shown in Figure 2. We have found that, depending on the type of surface under investigation, each of the formats shown can be useful in interpreting topographic data. The sample was the polished (210) surface of a single crystal of gold which was heated for a period of three minutes in situ to 850° several days before the picture was taken. We show an area 140 Å on a side, with 10 Å of vertical range. All of the pictures in this paper were obtained on the same surface with a similar heat treatment.

The pictures shown are generated by the Tektronix computer and take several seconds to produce. Figure 2(a) shows a projected line plot identical to that produced initially on the DEC LSI 11/23. The data have been rotated by 8° and 5° about the x- and y-axes, respectively, to make the plateaus appear flat for the viewer. Figures 2(b) and 2(c) are also projected plots, but now each rectangle on the data grid is shaded to indicate surface height. The range and intensity of the gray and color scales can easily be adjusted for greatest effectiveness. Figure 2(d) is a projected and filled plot with the gray level determined by the angle of the local surface normal with respect to a prechosen "light source" at infinity. The incident light in this picture is from the left at 90° to the viewing direction and 75° down from the vertical.

The viewing angles, in polar coordinates, for Figures 2(a)–(d) are $\theta = 30^{\circ}$ and $\Phi = 280^{\circ}$. Figure 2(e) presents the same data in top view. Here the x- and y-coordinates can be read directly from the abscissa and ordinate, while the height is determined by the shading. The top view is particularly useful for the determination of absolute distances between various surface features; for example, surface reconstructions. Finally, Figure 2(f) shows a single trace of the data, that is, the section in the x-z plane indicated by the arrow in Figure 2(a), clearly showing the atomic plateaus. The noise level in the z-direction is roughly 0.1 Å peak-topeak in a measurement bandwidth of several hundred Hz.

4. Instrument performance

Figure 3 demonstrates the ability of the microscope to "zoom in" on a particular feature, allowing the operator to search the surface for interesting regions. The resolution of the larger $4000\text{-}\text{Å} \times 4000\text{-}\text{Å}$ picture is limited by the data grid size to $16~\text{Å} \times 70~\text{Å}$, although this still permits observation of large distinguishing features. This picture took about 30 minutes to scan. Successive pictures in Figure 3 show rescans of portions of each preceding scan. The final images shown in Figures 3(e) and 3(f) comprise one percent of the initial area shown in Figure 3(a) and took roughly three minutes to scan.



Series of scans (projected view) of a polished gold $\langle 210 \rangle$ surface taken at a tip bias of $10 \, \mathrm{V}$ (a) and (b) are repeat scans taken three hours apart, (c) is an enlargement of the upper middle section of (b), (d) is from the lower left corner of (c), and (e) is from the upper middle section of (d). (f) is a rescan of (e), with a bias of $1.5 \, \mathrm{V}$.

unciear.

chance of the tip striking the surface during scanning, since the tip is further from the surface at higher bias voltage. At the end of the series the bias was reduced to 1.5 V, which both enhanced resolution substantially and changed some of the gross surface features. The reason for this change is as yet

5. Barrier height measurements

At lower bias voltages and currents, typically mV and nA, the STM operates in the tunneling regime. It has been suggested [5] that the tunneling current can be predicted by a simple WKB model of single-electron tunneling through a trapezoidal barrier. Such a picture predicts an exponential dependence of tunneling on tip-to-sample separation s. In this model, the tunneling current density j is given by

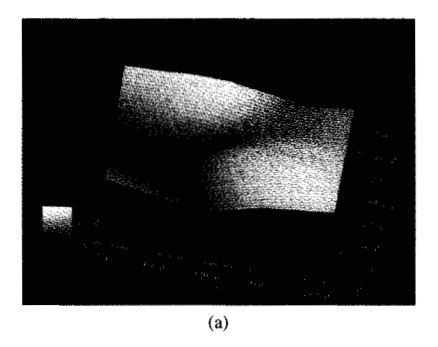
$$s\underline{\Phi m \zeta } (4/\zeta) - \frac{\partial}{\partial m} \underline{\Delta} \nabla \frac{1}{\sqrt{\zeta}} \left(\frac{1}{2} \right) = 0$$

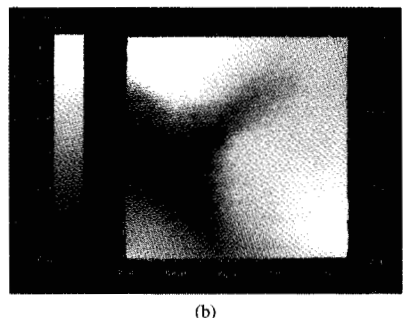
for a fixed bias voltage V (with $eV \ll \Phi$), where m is the

Needless to say, thermal drift is an important problem for the STM, since drift can distort pictures and interfere with reproducibility. Often, it is desirable to rescan a given area of such as bias voltage or ambient pressure. Figures 3(a) and 3(b) show the same region of the (210) surface of a single crystal of gold; they were obtained three hours apart. The pictures repeat rather well, and show a drift with respect to pictures repeat rather well, or 1 Å/min. This performance is typical of our instrument.

The first five pictures in Figure 3 were all taken with a bias The first five pictures in Figure 3 were all taken with a bias

of 10 V. At this high voltage, the signal/noise ratio of the current flowing between tip and sample was better than for the more usual bias voltages of 0.01 to 1 V, and large-area pictures with steep features were generally more reproducible. We attribute the improvement in current noise to a reduced sensitivity due to operation in the Fowler-Mordheim region, as opposed to the low-voltage tunneling regime. The improved reproducibility is due to a reduced





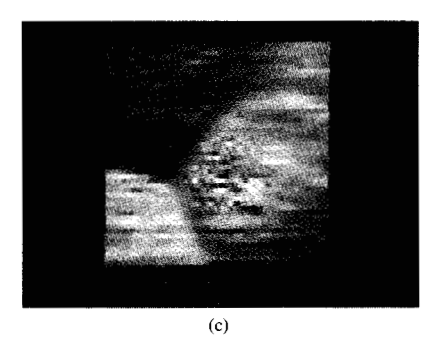


Figure 4

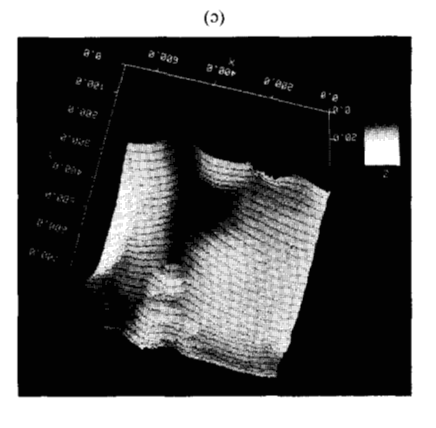
Data taken on a region of polished gold <210> surface, with tip bias of -50 mV. (a) and (b) are projected and top views, respectively, of surface topography. (c) is a top view of the effective barrier height as a function of position.

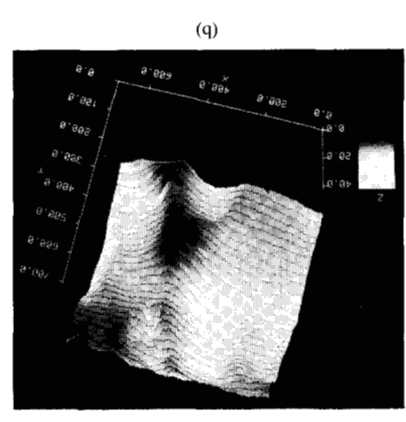
electron mass, h is Planck's constant, and Φ is the average work function of the tip and sample. If we neglect the image potential [6, 7], Φ is also the tunnel barrier height. For small variations in s, we can estimate the barrier height from $\partial(\ln I)/\partial s \approx 1.025\Phi^{1/2}$, with Φ in eV and s in Å, where I is the total tunneling current. We have produced maps of this model barrier height by sinusoidally modulating the tip-tosurface distance at a frequency higher than the roll-off frequency of the feedback loop, and detecting the modulation in the tunneling current with a lock-in amplifier [8]. Thus, by recording both the voltage applied to the z-drive and the output of the lock-in detector while the surface is scanned, we are able to obtain a "topographical map" and a "barrier height map" simultaneously. Figures 4(a) and (b) show topographic plots obtained at a bias of 50 mV for a 100-Å \times 100-Å region of the (210) surface of a gold sample that had been heated but not otherwise prepared. Figure 4(c) shows the barrier height map, obtained with a modulation frequency and peak-to-peak amplitude of 1 kHz and 0.4 Å, respectively. The gray scale in Figure 4(c) corresponds to an average barrier height that varies from 0.6 eV to 1.1 eV. These values, which are substantially lower than the work function of a clean gold surface [9], roughly 5 eV, are similar to those observed by other workers [10]. One should exercise caution in interpreting these potentials simply as work functions; nevertheless, it is reasonable to assume that the potentials in Figure 4(c) arise from variations in the work function of the surface, although the exact correspondence is far from clear. One sees that the Yshaped feature evident in Figures 4(a) and (b) is also shown very clearly in Figure 4(c). Furthermore, the three regions delineated by this feature appear to have different effective barrier heights. The fact that the effective barrier height varies with position implies that one should correct the "topographical map" for this variation.

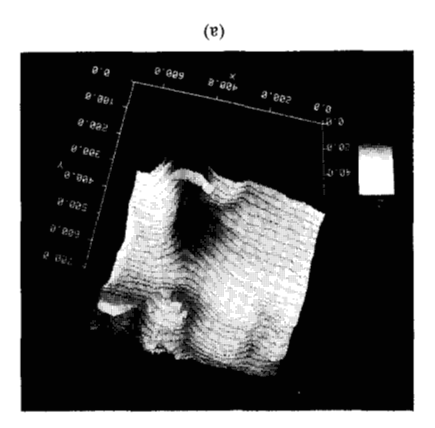
6. Surface modification

Our initial attempts at surface modification fall into two broad classes. First, we have touched the tip to the sample to produce scratches and indentations. Generally the resulting features are some 100 Å in size, although there is usually some deformation of the surface at distances of 500 Å or more from the primary indentation. Sometimes, however, we find that the tip has changed, so that the microscope is scanning a completely new section of the sample. Second, by working at high currents and small tip-to-sample separations we have deposited material from the tip onto the sample to produce hillocks typically 200 Å across. In both cases we have observed surface diffusion in the period following the initial formation. Reducing the current to 10 nA, and therefore increasing the spacing, s, ensured that the scanning process did not significantly affect the diffusion process.

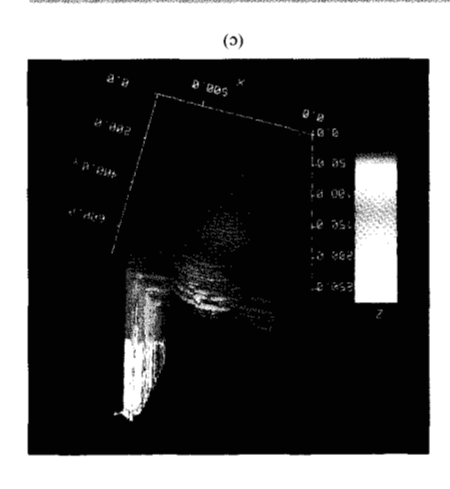
The effect of lowering the tip onto the gold sample is shown in Figure 5. Initially, the surface was featureless. The tip was moved to the center of the picture, and the tunneling resistance was reduced to about 200 Ω for several seconds. This 200 Ω is presumably contact resistance, and roughly agrees with an estimate based on the observed contact area. The center portion of the resulting hole [Figure 5(a)] was more or less axially symmetric in shape and was approximately 150 Å across and 30 Å deep. In addition, we found that the surface was deformed to some extent over a region roughly 700 Å across. After $3\frac{1}{2}$ minutes had elapsed, some of these latter irregularities had annealed out [Figure 5(b)]; after a further $13\frac{1}{5}$ minutes the stable configuration shown in Figure 5(c) was reached. Subsequent pictures showed no significant changes in the structure. The final result is a very well-defined Y-shaped pattern roughly 10 Å deep, and is very similar to the naturally occurring feature seen in Figure 4. We speculate that this pattern may be caused by stress relief in the gold surface. The total spatial

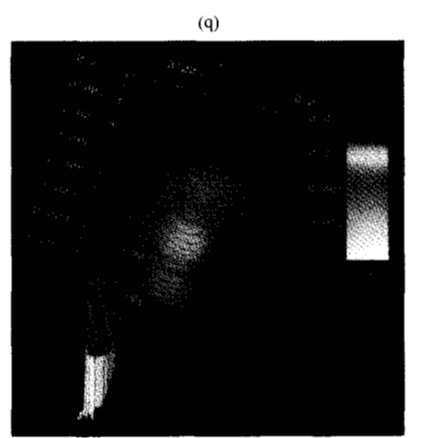


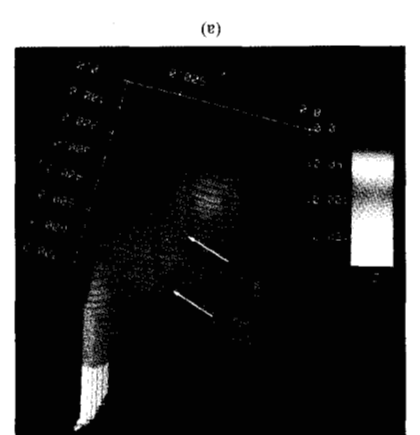




Series of images (projected view) taken after lowering the tip onto the surface. (a) was taken immediately afterwards, (b) $3^{1/2}$ minutes later, and (c) after another $13^{1/2}$ minutes.







Sequence of images (projected view) showing deposition of material onto surface. (a) was taken just prior to the formation of hillocks seen in (b); (c) was taken 12 minutes after (b).

While there are several possibilities, we think that these hillocks were formed by the deposition of material from the tip onto the surface. In its previous history, the tungsten tip had touched the gold surface many times, and it seems likely that a small amount of gold was transferred to the tip. The mechanism for the transfer of gold back to the surface during deposition is as yet unclear. Simple estimates based on the power dissipated in the junction between tip and sample suggest that significant heating did not occur. Thus, it seems likely that material was transferred due to the close it seems likely that material was transferred due to the close or the close that the transferred are the sample.

In contrast to the deformation experiments illustrated in Figure 5, the deposition procedure appears to be very local,

extent of the disturbance from this process seems to be at least 500 Å square, even for extremely delicate contact. In the second experiment (Figure 6) we produced hillocks

on the surface by increasing the tunneling current to 1 μ A with the tip biased at +5 mV. We were also able to form hillocks with the tip negative. Initially, the surface of the sample was relatively flat with a sharply rising feature at the confirm that subsequent scans were made over exactly the same region. In the experiment illustrated here, we produced two hillocks at the positions indicated by arrows in Figure 6(a). Initially the hillocks were counded in shape and were two hillocks at the positions indicated by arrows in Figure 6(a). Initially the hillocks were rounded in shape and were

and not to disturb a larger surrounding area: For example, in Figures 6(a), (b), and (c) the small feature roughly 250 Å to the left of the hillocks was unaffected by the deposition process. Subsequent pictures showed that the hillocks diffused laterally. In Figure 6(c), taken 12 minutes after Figure 6(b) was obtained, the diffusion process appears to have been completed; the hillocks have developed flat tops and are now roughly 300 to 400 Å across and 12 Å high. A literal interpretation of Figures 6(b) and (c) as topographical maps would suggest that the volume of the hillocks increased by about 50%. However, one should not rule out the possibility that the effective barrier height of the freshly deposited material might have changed with time, thereby giving rise to an incorrect relative height measurement. It would obviously be of interest to make simultaneous barrier height and topographic maps of deposited material.

These experiments have wide-ranging implications in the study of surface diffusion, hardness measurements on a nanometer scale, and micro-machining. In addition, the techniques outlined are potentially useful as a mechanism for high-density memory storage [11]. Finally, it would be particularly interesting to see if one could obtain atomic resolution after procedures of these kinds.

7. Summary

We have constructed an STM that has a thermal drift rate of 1 Å/min or less after a stabilization period of a few hours. This very low drift rate enables us to "zoom in" on a small region of a much larger scan. Samples can be removed from the microscopes for in situ surface preparation and analysis, and subsequently remounted. A variety of graphics options are available to enable us to present the data in the most advantageous manner. We are able to make scans of topography and barrier height simultaneously; features observed in the topography are often visible in the barrier height maps. By lowering the tip to the surface we have been able to produce indentations typically 100 Å across; however, the surface is often distorted over distances up to 500 Å from the indentation. By operating the microscope at a high tunneling current (1 μ A) and reduced gap spacing, we have been able to deposit material on the surface to form hillocks roughly 300 to 400 Å across and 12 Å high. In both surface-modification processes, surface diffusion was observed with a characteristic time of the order of minutes.

Acknowledgments

We would like to acknowledge useful discussions with G. Binnig, S. Chiang, J. A. Golovchenko, H. Rohrer, C. Quate, and R. Wilson. We would also like to thank C. Barr and F. Ogletree for generously supplying gold samples. One of us (E. G.) gratefully acknowledges the receipt of an IBM Predoctoral Fellowship. This work was supported by the Director, Office of Energy Research, Office

of Basic Energy Science, Material Science Division of the U.S. Department of Energy, under Contract No. DE-AC03-76SF-00098.

References and note

- 1. G. Binnig and H. Rohrer, Surf. Sci. 126, 236 (1983).
- Electron Microscopy and Analysis, 1981, M. J. Goringe, Ed., The Institute of Physics, London, 1981.
- Philip F. Kane, Characterization of Solid Surfaces, Philip F. Kane and Graydon B. Larabee, Eds., Plenum Press, New York, 1978, p. 133.
- H. Jonathon Mamin, David W. Abraham, Eric Ganz, and John Clarke, Rev. Sci. Instrum. 56, 2168 (1985).
- 5. J. G. Simmons, J. Appl. Phys. 34, 1793 (1963).
- 6. J. G. Simmons, J. Appl. Phys. 35, 2472 (1964).
- S. Elrod, Ph.D. Thesis, Stanford University, Stanford, CA, 1985. Inclusion of the image potential can reduce the effective barrier height to as much as 1 V below the average work function, for tip-to-sample spacings less than 10 Å.
- G. Binnig, H. Rohrer, Ch. Gerber, and E. Weibel, *Phys. Rev. Lett.* 49, 57 (1982).
- 9. E. E. Huber, Jr., Appl. Phys. Lett. 8, 169 (1966).
- Private communications with G. Binnig (IBM Research Division, Zurich, Switzerland), J. A. Golovchenko (AT&T Laboratories, Holmdel, NJ), and Prof. C. Quate (Stanford University, Stanford, CA).
- 11. Prof. C. Quate, private communication.

Received September 19, 1985; accepted for publication October 21, 1985

David W. Abraham Lawrence Berkeley Laboratory, Center for Advanced Materials, Berkeley, California 94720. Dr. Abraham received his Ph.D. in 1983 from Harvard University, Cambridge, Massachusetts, where he studied phase transitions in two-dimensional superconducting films. He is currently a Postdoctoral Fellow at the Center for Advanced Materials.

H. Jonathon Mamin Lawrence Berkeley Laboratory, Center for Advanced Materials, Berkeley, California 94720. Dr. Mamin received his Ph.D. in 1984 from the University of California, Berkeley. His work centered on the study of thermally induced charge imbalance in superconducting aluminum. Dr. Mamin is a Postdoctoral Fellow at the Center for Advanced Materials.

Eric Ganz University of California, Department of Physics, Berkeley, California 94720. Mr. Ganz received his B.S. from Stanford University, Stanford, California, in 1982, and is currently a graduate student in the Physics Department at the University of California, Berkeley.

John Clarke University of California, Department of Physics, Berkeley, California 94720. Professor Clarke is a Professor of Physics at the University of California, Berkeley, and a Principal Investigator at the Lawrence Berkeley Laboratory. He is known for his work in the development of superconducting quantum interference devices (SQUIDs).

DAVID W. ABRAHAM ET AL.